

Long non-coding RNA OIP5-AS1 contributes to cisplatin resistance of oral squamous cell carcinoma through the miR-27b-3p/TRIM14 axis

ZHEN XIAO^{1,2}, JIAYI LI³, QINGSONG JIN¹ and DONGXIU LIU⁴

¹Oral and Maxillofacial Second Ward, The First Hospital of Qiqihar;

²Department of Stomatology, Affiliated Qiqihar Hospital, Southern Medical University;

³Department of Stomatology, The Third Affiliated Hospital of Qiqihar Medical University, Qiqihar, Heilongjiang 161000;

⁴Department of Stomatology, The Fourth People's Hospital of Shaanxi, Xi'an, Shaanxi 710043, P.R. China

Received October 10, 2019; Accepted September 18, 2020

DOI: 10.3892/etm.2021.9839

Abstract. Oral squamous cell carcinoma (OSCC) accounts for 90% of oral cavity cancer types, but the overall prognosis for patients with OSCC remains unfavorable. Cisplatin (DDP) is an effective drug in OSCC treatment, but DDP resistance weakens its therapeutic effect. Opa-interacting protein 5 antisense RNA 1 (OIP5-AS1) can trigger DDP resistance. The purpose of the current study was to explore the role and mechanism of OIP5-AS1 in OSCC DDP resistance. In the present study, the expression levels of OIP5-AS1, microRNA (miR)-27b-3p and tripartite motif-containing 14 (TRIM14) were detected by reverse transcription-quantitative PCR. DDP resistance was measured using an MTT assay. Moreover, cell proliferation, migration and invasion were assessed by MTT, Transwell, and Matrigel assays. Protein expression levels of TRIM14, E-cadherin, N-cadherin and Vimentin were detected by western blot analysis. Putative binding sites between miR-27b-3p and OIP5-AS1 or TRIM14 were predicted with starBase and verified using a dual-luciferase reporter assay. The role of OIP5-AS1 in DDP resistance of OSCC *in vivo* was measured using a xenograft tumor model. It was observed that OIP5-AS1 was upregulated in DDP-resistant OSCC cells, and the knockdown of OIP5-AS1 improved DDP sensitivity in DDP-resistant OSCC cells. The present study identified that miR-27b-3p was a target of OIP5-AS1. Furthermore, miR-27b-3p silencing reversed the effect of OIP5-AS1 knockdown on DDP sensitivity in DDP-resistant OSCC cells. TRIM14 was shown to be a direct target of

miR-27b-3p, and TRIM14 overexpression abolished the effect of miR-27b-3p on DDP sensitivity in DDP-resistant OSCC cells. The results suggested that OIP5-AS1 increased TRIM14 expression by sponging miR-27b-3p. In addition, OIP5-AS1 knockdown enhanced DDP sensitivity of OSCC *in vivo*. Data from the present study indicated that OIP5-AS1 may improve DDP resistance through the upregulation of TRIM14 mediated by miR-27b-3p, providing a possible therapeutic strategy for OSCC treatment.

Introduction

Oral cavity cancer is an intractable malignancy that has become a highly relevant public health issue worldwide (1). According to global cancer statistics from 2018, there were ~354,864 newly diagnosed cases and 177,384 mortalities of oral cavity cancer (2). Furthermore, >90% of oral cavity cancer types are identified as oral squamous cell carcinoma (OSCC) (3). Although great progress has been made in diagnosis, surgery and chemotherapy strategies, the overall prognosis of OSCC remains unfavorable owing to local recurrence and metastasis (4). Cisplatin (DDP) has been reported as an effective first-line chemotherapy drug for the treatment of OSCC, but the therapeutic effect of DDP often fails as a result of the rapid development of drug resistance (5). Thus, it is important to identify the underlying molecular mechanisms of chemoresistance in OSCC to develop a novel target for improving DDP sensitivity.

Long non-coding RNAs (lncRNAs) are >200 nucleotides and have been identified as crucial regulatory transcripts lacking protein-coding functions (6). Previous studies have reported that dysregulation of lncRNAs is implicated in the initiation and development of various tumors, including OSCC (7,8). LncRNA opa-interacting protein 5 antisense RNA 1 (OIP5-AS1) is derived from the antisense of OIP5 gene; it acts as a carcinogenic factor by promoting cell proliferation, migration and invasion in OSCC progression (9). Moreover, a recent study observed that OIP5-AS1 could induce DDP resistance by regulating microRNA (miRNA/miR)-340-5p in osteosarcoma (10). ever, the function and mechanism of

Correspondence to: Dr Dongxiu Liu, Department of Stomatology, The Fourth People's Hospital of Shaanxi, 512 Xianning East Road, Xi'an, Shaanxi 710043, P.R. China
E-mail: yihao20072@yeah.net

Key words: opa-interacting protein 5 antisense RNA 1, microRNA-27b-3p, tripartite motif-containing 14, cisplatin, oral squamous cell carcinoma

OIP5-AS1 in DDP-resistant OSCC cells are yet to be fully elucidated.

In recent decades, miRNAs (small non-coding RNAs ~22 nucleotides in length) have been reported to negatively regulate gene expression in part by repressing translation of target mRNAs (11). Numerous miRNAs have been found to be abnormally expressed and closely associated with physiological activities, including proliferation, metastasis and development in OSCC (12-14). miR-27b-3p, a form of mature miR-27b, has been revealed to exert a tumor-suppressive effect by regulating its target genes, including MET and frizzled class receptor 7 in OSCC (15,16). Previous studies have suggested that miR-27b-3p could reduce resistance of some drugs in breast cancer and prostate cancer (17,18). In addition, a recent study reported that miR-27b could improve the chemotherapy sensitivity of OSCC cells to DDP (19), indicating the involvement of miR-27b-3p in DDP resistance of OSCC.

Tripartite motif-containing 14 (TRIM14), located on chromosome 9q22, was first identified in HIV-infected human and simian lymphomas (20). It has been shown that TRIM14 is upregulated in OSCC, and the overexpression of TRIM14 could facilitate the progression of OSCC by interacting with miR-195-5p (21). Furthermore, previous studies have demonstrated that TRIM14 contributes to drug resistance in gliomas and oral tongue squamous cell carcinoma (22,23). However, the involvement of TRIM14 in DDP-resistant in OSCC remains unknown.

Therefore, the aim of the present study was to identify the function of OIP5-AS1, and to explore whether the involvement of OIP5-AS1 in the DDP resistance of OSCC was mediated via the miR-27b-3p/TRIM14 axis.

Materials and methods

Clinical samples and cell culture. Samples of OSCC tumor tissues and normal adjacent tissues (the distance from the tumor margin was >5 cm) were collected from 30 patients (17 male and 13 females; 12 patients aged >60 and 18 patients aged <60; age range, 27-78 years) who underwent oral surgical operation at The First Hospital of Qiqihar (Qiqihar, China) from January 2015 to June 2017. Tissues excised during the surgery were instantly frozen in liquid nitrogen and stored at -80°C until subsequent use. The study was performed with the approval of the Ethical Committee of The First Hospital of Qiqihar. Written informed consent was obtained from all participating patients.

A normal human oral keratinocyte cell line (NHOK) was obtained from the Cell Bank of Type Culture Collection of the Chinese Academy of Sciences (Shanghai, China) and incubated in Keratinocyte-SFM medium (Invitrogen; Thermo Fisher Scientific, Inc.) containing 10% FBS (Invitrogen; Thermo Fisher Scientific, Inc.) and 1% antibiotics (100 U/ml penicillin and 100 µg/ml streptomycin; Invitrogen; Thermo Fisher Scientific, Inc.) in a 5% CO₂ incubator at 37°C. Human OSCC cell lines (SCC-15, SCC-9 and Cal-27) were purchased from the American Type Culture Collection, and the human OSCC cell line HSC-3 was acquired from Cell Bank of Japanese Collection of Research Bioresources. All OSCC cells were cultured at 37°C with 5% CO₂ under a humid atmosphere in DMEM (Invitrogen; Thermo Fisher Scientific, Inc.)

supplemented with 10% FBS (Gibco; Thermo Fisher Scientific, Inc.).

A gradually increasing dose of DDP (from 1.5 to 25 µg/ml over a 10-month period; Sigma-Aldrich; Merck KGaA) at 37°C was added to the culture medium of SCC-9/DDP and HSC-3/DDP cells for maintaining the DDP-resistant phenotype, as previously described (24).

Cell transfection. OIP5-AS1 or TRIM14 overexpression vectors were established by inserting OIP5-AS1 or TRIM14 cDNA sequence into pcDNA3.1 (pcDNA; Invitrogen; Thermo Fisher Scientific, Inc.), obtaining pcDNA-OIP5-AS1 or pcDNA-TRIM14. And the pcDNA3.1 empty vector (pcDNA; Invitrogen; Thermo Fisher Scientific, Inc.) acted as a negative control. Small interfering (si)RNA against OIP5-AS1 (si-OIP5-AS1: 5'-GGCAGTAGAATCACTTAA-3') and its scrambled negative control (si-NC: 5'-TACCGACTGGCAATTCATG-3'), miR-27b-3p mimic (miR-27b-3p: 5'-TTCACAGTGGCTAAGTTCTG-3') and miR-27b-3p inhibitor (anti-miR-27b-3p: 5'-GCAGAACTTAGCCACTGTGAA-3'), as well as their scrambled NC (miR-NC: 5'-GGTTCATC GTACACTGTTCA-3' or anti-miR-NC: 5'-CCATCAGTCCCCATCGCCA-3') were obtained from Shanghai GenePharma Co., Ltd. Transfection of all aforementioned plasmids or oligonucleotides was performed in OSCC cells (2x10⁵ cells/well) using Lipofectamine® 2000 reagent (Invitrogen; Thermo Fisher Scientific, Inc.), according to the manufacturer's instructions. After 48 h incubation at 37°C, transfected cells were harvested and utilized for further experiments.

Reverse transcription-quantitative PCR (RT-qPCR). Extraction of RNA from OSCC tissues and cells was conducted using TRIzol® reagent (Gibco; Thermo Fisher Scientific, Inc.) according to the manufacturer's protocol. cDNA was synthesized using PrimeScript™ RT Master mix kit (Takara Bio, Inc.), followed by incubation at 37°C for 15 min and 85°C for 5 sec. Relative expression levels of OIP5-AS1 and TRIM14 were analyzed using the SYBR® Premix Ex Taq™ kit (Takara Bio, Inc.), and the amplification parameters were: Denaturation at 95°C for 10 min, followed by 40 cycles of denaturation at 95°C for 30 sec, annealing at 60°C for 30 sec and extension at 72°C for 1 min. The quantitative analysis of miR-27b-3p was performed using an All-in-One™ miRNA RT-qPCR Detection kit (GeneCopoeia, Inc.), and the PCR cycling profile was as follows: Denaturation at 95°C for 2 min; followed by 40 cycles of annealing at 95°C for 5 sec; and extension at 60°C for 35 sec. Subsequently, the expression levels of OIP5-AS1, miR-27b-3p and TRIM14 were calculated using 2^{-ΔΔCq} method (25), normalizing to GAPDH or U6 small nuclear RNA. The specific primer sequences used were as follows: OIP5-AS1 forward, 5'-TGCGAAGATGGC GGAGTAAG-3' and reverse, 5'-TAGTTCCTCTCTCTGGC CG-3'; miR-27b-3p forward, 5'-ACACTCCAGCTGGGTTTC ACAGTGGCTAAG-3' and reverse, 5'-TGGTGTCGTGGA GTCG-3'; TRIM14 forward, 5'-GCAGAGACAGAGCTAGAC TGTAAGGT-3' and reverse, 5'-CCTGGTCAACAATT GATATGGA-3'; GAPDH forward, 5'-AGAAGGCTGGGG CTCATTG-3' and reverse, 5'-AGGGGCCATCCACAGTCT TC-3'; and U6 forward, 5'-CTCGCTTCGGCAGCACA-3' and reverse, 5'-AACGCTTCACGAATTTGCGT-3'.

Drug resistance assay and cell proliferation assay. An MTT assay (Sigma-Aldrich; Merck KGaA) was performed to measure DDP resistance and cell proliferation, according to the manufacturer's instructions. Transfected DDP-resistant OSCC cells were cultured at 37°C for 48 h prior to exposure to different doses of DDP (1, 2, 4, 6, 8, 16, 32 and 64 $\mu\text{g/ml}$), and then the MTT assay was performed. The IC_{50} was calculated using a viability curve.

For the proliferation assay, transfected DDP-resistant OSCC cells (6×10^3 cells/well) were incubated for 48 h, and then 20 μl MTT solution (5 mg/ml) was added to each well at the different time points (0, 24, 48 and 72 h), followed by incubation for another 4 h at 37°C. After removing the cell culture medium, 100 μl DMSO (Sigma-Aldrich; Merck KGaA) was added into each well. The optical density (OD) was detected with a microplate reader at 490 nm (ELX808; BioTek Instruments, Inc.).

Cell migration and invasion assay. The cell migratory and invasive abilities were detected using Transwell chambers (24-well; Sigma-Aldrich; Merck KGaA) according to the manufacturer's instructions. Transfected SCC-9/DDP and HSC-3/DDP cells (1×10^6) were inoculated into the upper chamber with serum-free medium for migration assay. In total, 5×10^4 transfected DDP-resistant OSCC cells were added into the upper chamber coated with Matrigel at 37°C for 4–5 h (BD Biosciences) for the invasion assay. The lower chamber contained complete medium with 10% FBS (Gibco; Thermo Fisher Scientific, Inc.). After 24 h of incubation, the cells on the surface of the upper chamber were scraped with cotton swabs, whereas cells that migrated or invaded to the lower chamber were fixed with methanol for 30 min at 4°C and stained with 0.1% crystal violet solution for 20 min at 37°C. Cells were analyzed with an inverted fluorescent microscope (magnification, $\times 100$).

Western blot analysis. Western blotting was conducted according to previous description (26). Total protein from tissues and cells was isolated using pre-cold RIPA buffer (Beyotime Institute of Biotechnology) including protease inhibitor. Total protein was quantified using a BCA protein assay kit (Invitrogen; Thermo Fisher Scientific, Inc.). Separated proteins (30 μg) using 10% SDS-PAGE were transferred onto nitrocellulose membranes (EMD Millipore). The membranes were probed with primary antibodies against TRIM14 (1:800; cat. no. ab185349; Abcam), E-cadherin (1:1,000; cat. no. ab1416; Abcam), N-cadherin (1:1,000; cat. no. ab76011; Abcam), Vimentin (1:200; cat. no. ab8978; Abcam) and GAPDH (1:5,000; cat. no. ab9485; Abcam) at 4°C overnight. Subsequently, the corresponding horseradish peroxidase conjugated goat-anti-rabbit secondary antibody (1:10,000; cat. no. ab205178, Abcam) was probed in the membranes to bind these primary antibodies. Protein bands were detected with an ECL detection system (Cytiva) and analyzed using Quantity One v4.6.2 software (Bio-Rad Laboratories, Inc.). And the expression levels of protein were normalized to GAPDH.

Dual-luciferase reporter assay. Using the bioinformatics website starBase v2.0 (<http://starbase.sysu.edu.cn/agoClipRNA.php?source=IncRNA>), the binding sites between the miR-27b-3p and OIP5-AS1 or TRIM14 3'-untranslated regions (UTR) were predicted and analyzed. A luciferase activity reporter assay was conducted to further assess the binding relationship between miR-27b-3p and OIP5-AS1 or TRIM14 3'-UTR. Partial sequences of OIP5-AS1 and TRIM14 3'-UTR containing the putative (wild-type; WT) or mutated putative binding sites for miR-27b-3p were amplified and cloned into psiCHECK-2 vector (Promega Corporation), resulting in OIP5-AS1 WT or MUT and TRIM14 3'-UTR WT or MUT reporter plasmids. Then, SCC-9/DDP and HSC-3/DDP cells (2×10^5 cells/well) were co-transfected with 100 ng of the constructed reporter plasmids and 100 nM miR-NC or miR-27b-3p and were incubated for 48 h at 37°C. Luciferase activities were measured with the LD400 luminometer (Beckman Coulter, Inc.) at 48 h post-transfection. Firefly luciferase activity was normalized to that of *Renilla* luciferase.

cn/agoClipRNA.php?source=IncRNA), the binding sites between the miR-27b-3p and OIP5-AS1 or TRIM14 3'-untranslated regions (UTR) were predicted and analyzed. A luciferase activity reporter assay was conducted to further assess the binding relationship between miR-27b-3p and OIP5-AS1 or TRIM14 3'-UTR. Partial sequences of OIP5-AS1 and TRIM14 3'-UTR containing the putative (wild-type; WT) or mutated putative binding sites for miR-27b-3p were amplified and cloned into psiCHECK-2 vector (Promega Corporation), resulting in OIP5-AS1 WT or MUT and TRIM14 3'-UTR WT or MUT reporter plasmids. Then, SCC-9/DDP and HSC-3/DDP cells (2×10^5 cells/well) were co-transfected with 100 ng of the constructed reporter plasmids and 100 nM miR-NC or miR-27b-3p and were incubated for 48 h at 37°C. Luciferase activities were measured with the LD400 luminometer (Beckman Coulter, Inc.) at 48 h post-transfection. Firefly luciferase activity was normalized to that of *Renilla* luciferase.

Tumor xenograft assay. Male BALB/C nude mice (n=6 per group; age, 4 weeks, 18–20 g weight) were obtained from the Shanghai Experimental Animal Center. A total of 12 mice were kept in an environmental room equipped with a constant temperature of 20°C, a humidity of 60% and a programmed 12 h light/dark cycle for circadian control, and were randomly divided into 2 groups (the sh-NC+cisplatin group, and the sh-OIP5-AS1+cisplatin). All mice were allowed free access to drinking water and sterilized standard diet. The animal experiment was performed as per the protocol approved by the Institutional Committee for Animal Research of The First Hospital of Qiqihar. The short hairpin (sh)-OIP5-AS1 lentivirus was obtained from Shanghai GenePharma Co., Ltd, and a lentivirus empty vector was used as the sh-NC. Subsequently, these obtained lentivirus vectors were transfected into 293T cells (Invitrogen; Thermo Fisher Scientific, Inc.) along with lentivirus packaging vectors (psPAX2 and pMD2. G, Addgene, Inc.), followed by incubation for 72 h at 37°C. After collection with cell supernatants including sh-OIP5-AS1 or sh-NC lentivirus, SCC-9 cells were infected with sh-OIP5-AS1 or sh-NC lentivirus, followed by screening with puromycin (Sigma-Aldrich; Merck KGaA). One week later, stable lentivirus-transfected SCC-9 cells were established. Subsequently, transfected cells (5×10^6) were subcutaneously injected into the left flank of the nude mice. At 7 days after injection, 3 mg/kg DDP (dissolved in PBS buffer; Sigma-Aldrich; Merck KGaA) was intraperitoneally injected once every 4 days. Tumor volume was measured every 4 days after the first injection (the largest tumor diameter was 128 mm). After 31 days, mice were euthanized by the administration of 5% isoflurane followed by cervical dislocation. Tumors were excised, weighed, and were stored at -80°C for subsequent experiments.

Statistical analysis. GraphPad Prism 7.0 software (GraphPad Software, Inc.) was used for statistical analysis. Paired Student's t-test or one-way ANOVA with Tukey's tests were used to analyze the differences in the data between two groups or among multiple groups, respectively. The correlation between OIP5-AS1, miR-27b-3p and TRIM14 was detected using Pearson's correlation analysis. Data are presented as the mean \pm SD. $P < 0.05$ was considered to indicate a statistically significant difference.

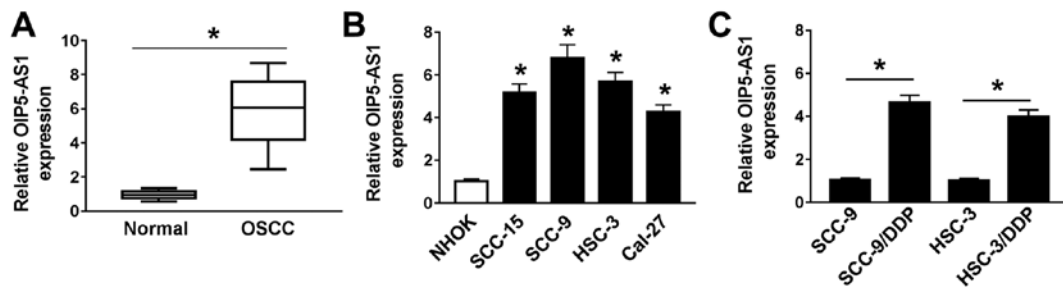


Figure 1. OIP5-AS1 expression is upregulated in OSCC tissues and cells, as well as DDP-resistant OSCC cells. (A) RT-qPCR was performed to measure the expression levels of OIP5-AS1 in 30 pairs of OSCC tumor tissues and normal adjacent tissues. * $P < 0.05$. (B) OIP5-AS1 expression was detected in OSCC cell lines (SCC-15, SCC-9, HSC-3 and Cal-27) and NHOK cells. * $P < 0.05$ vs. NHOK. (C) Expression of OIP5-AS1 in OSCC cell lines (SCC-9 and HSC-3) and DDP-resistant OSCC cell lines (SCC-9/DDP and HSC-3/DDP) was assessed by RT-qPCR assay. * $P < 0.05$. DDP, cisplatin; NHOK, normal human oral keratinocyte; OIP5-AS1, opa-interacting protein 5 antisense RNA 1; OSCC, oral squamous cell carcinoma; RT-qPCR, reverse transcription-quantitative PCR.

Results

OIP5-AS1 is upregulated in OSCC tissues and cells, as well as DDP-resistant OSCC cells. To investigate the function of OIP5-AS1 with DDP resistance in OSCC, its expression was first measured by RT-qPCR assay. OIP5-AS1 expression was significantly increased in OSCC tissues in comparison with normal adjacent tissues ($n=30$; Fig. 1A). Similarly, significantly higher expression of OIP5-AS1 was observed in OSCC cell lines (SCC-15, SCC-9, HSC-3 and Cal-27) compared with NHOK cells (Fig. 1B), most notably in SCC-9 and HSC-3 cells. Thus, SCC-9 and HSC-3 cells were selected for the subsequent analyses.

OIP5-AS1 expression in DDP-resistant OSCC cells was further examined. The results demonstrated that OIP5-AS1 expression was significantly upregulated in SCC-9/DDP and HSC-3/DDP cells compared with their respective parental cells SCC-9 and HSC-3 (Fig. 1C). These data suggested that dysregulation of OIP5-AS1 maybe associated with DDP resistance in OSCC cells.

OIP5-AS1 knockdown improves DDP sensitivity in DDP-resistant OSCC cells. Considering the high expression of OIP5-AS1 in DDP-resistant OSCC cells, OIP5-AS1 was knocked down in SCC-9/DDP and HSC-3/DDP cells. The expression of OIP5-AS1 was effectively downregulated in SCC-9/DDP and HSC-3/DDP cells transfected with si-OIP5-AS1 compared with cells with si-NC (Fig. 2A). Therefore, this knockdown vector was used to further evaluate the effect of OIP5-AS1 on DDP resistance in DDP-resistant OSCC cells. The drug cytotoxicity assay results suggested that the IC_{50} value of DDP in si-OIP5-AS1-transfected DDP-resistant OSCC cells was significantly decreased compared with the respective si-NC-transfected DDP-resistant OSCC cells (Fig. 2B-D), indicating that the OIP5-AS1 knockdown could reduce the resistance of the cells to DDP.

Functional analysis suggested that OIP5-AS1 knockdown significantly repressed proliferation (Fig. 2E and F), migration (Fig. 2G) and invasion (Fig. 2H) in SCC-9/DDP and HSC-3/DDP cells. Moreover, western blot analysis revealed that OIP5-AS1 knockdown significantly increased E-cadherin protein expression, but decreased N-cadherin and Vimentin protein expression levels, indicating that the knockdown of OIP5-AS1 may suppress epithelial-mesenchymal transition (EMT) in SCC-9/DDP and HSC-3/DDP cells (Fig. 2I and J).

Collectively, these data demonstrated that OIP5-AS1 knockdown could decrease DDP resistance, and inhibit cell growth and metastasis in SCC-9/DDP and HSC-3/DDP cells.

miR-27b-3p directly interacted with OIP5-AS1. lncRNAs can exert their function by interacting with miRNAs (27). Hence, the underlying interacting miRNAs of OIP5-AS1 were predicted using starBase v2.0 software, and miR-27b-3p was found to possess complementary sites with OIP5-AS1 (Fig. 3A). The dual luciferase reporter assay was used to further verify this predicted outcome. It was demonstrated that miR-27b-3p overexpression significantly decreased the luciferase activity of OIP5-AS1 WT reporter plasmid, but had no notable effect on the luciferase activity of OIP5-AS1 MUT reporter plasmid in SCC-9/DDP and HSC-3/DDP cells (Fig. 3B and C).

miR-27b-3p was demonstrated to be expressed at significantly lower levels in OSCC tumors and cell lines compared with the respective control groups (Fig. 3D and E). In addition, the expression of miR-27b-3p was moderately negatively correlated with OIP5-AS1 expression in OSCC tumors (Fig. 3F) (28). The transfection efficiency of pcDNA-OIP5-AS1 overexpression vector in SCC-9/DDP and HSC-3/DDP cells was detected (Fig. 3G). RT-qPCR results showed that miR-27b-3p expression was increased in si-OIP5-AS1-transfected DDP-resistant OSCC cells but was decreased in pcDNA-OIP5-AS1-transfected cells (Fig. 3H). Thus, it was indicated that OIP5-AS1 interacted with miR-27b-3p to hinder its expression.

OIP5-AS1 knockdown increases DDP sensitivity in DDP-resistant OSCC cells by negatively regulating miR-27b-3p. As an interaction between OIP5-AS1 and miR-27b-3p in DDP-resistant OSCC cells was indicated, it was further investigated whether the effect of OIP5-AS1 on DDP resistance was associated with miR-27b-3p. Knockdown of OIP5-AS1 could upregulate miR-27b-3p expression, which was subsequently downregulated after co-transfection with anti-miR-27b-3p (Fig. 4A). Furthermore, the results of IC_{50} determination suggested that the silencing of miR-27b-3p partly abolished the inhibitory effect of OIP5-AS1 knockdown on DDP resistance in SCC-9/DDP and HSC-3/DDP cells (Fig. 4B-D).

Functionally, the knockdown of OIP5-AS1 inhibited proliferation (Fig. 4E and F), migration (Fig. 4G), and invasion (Fig. 4H) in SCC-9/DDP and HSC-3/DDP cells, while miR-27b-3p silencing significantly reversed the suppressive

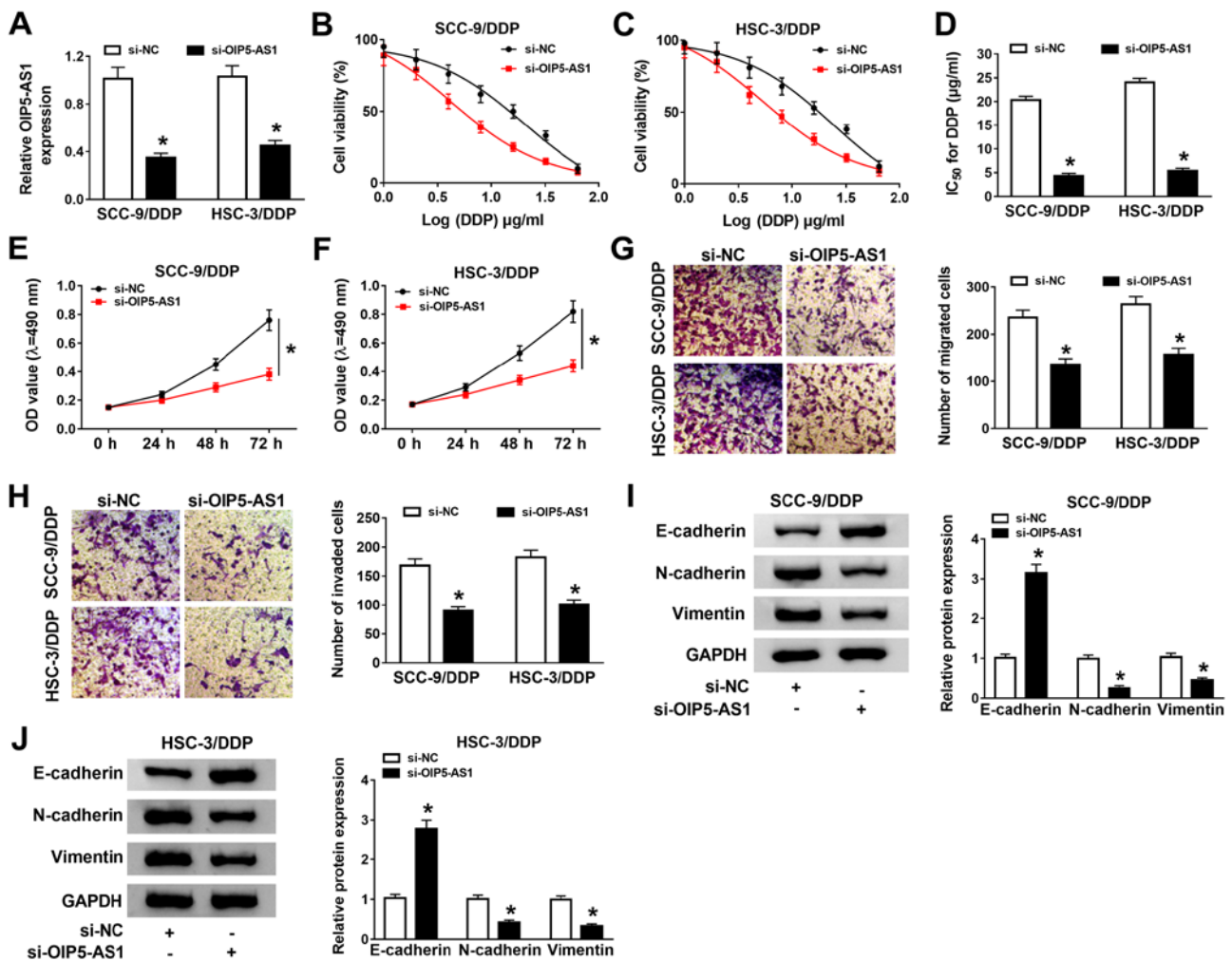


Figure 2. OIP5-AS1 knockdown enhances DDP sensitivity in DDP-resistant OSCC cells. (A) OIP5-AS1 expression in SCC-9/DDP and HSC-3/DDP transfected with si-OIP5-AS1 was detected using RT-qPCR analysis. (B and C) SCC-9/DDP and HSC-3/DDP cells transfected with si-OIP5-AS1 were treated with different concentrations of DDP for 48 h, and then cell viability was detected by using MTT assay. (D) The IC₅₀ was calculated using a viability curve. Proliferation rates were analyzed by MTT assay in si-OIP5-AS1-transfected (E) SCC-9/DDP and (F) HSC-3/DDP cells. (G) Migration and (H) invasion were analyzed with Transwell and Matrigel assays (magnification, x100), respectively, in si-OIP5-AS1-transfected DDP-resistant OSCC cells. Epithelial-mesenchymal-transition-related protein expression levels (E-cadherin, N-cadherin and Vimentin) were detected by western blot analysis in si-OIP5-AS1-transfected (I) SCC-9/DDP and (J) HSC-3/DDP cells. *P<0.05 vs. si-NC. DDP, cisplatin; NC, negative control; OD, optical density; OIP5-AS1, opa-interacting protein 5 antisense RNA 1; OSCC, oral squamous cell carcinoma; RT-qPCR, reverse transcription-quantitative PCR; siRNA, small interfering RNA.

effect of si-OIP5-AS1 on these biological processes. Meanwhile, cell images of the migration and invasion assays were presented in Fig. S2A and B. Western blotting results demonstrated that silencing of miR-27b-3p reversed the si-OIP5-AS1-induced enhancement in E-cadherin protein expression, as well as the reduction in N-cadherin and Vimentin protein expression levels in SCC-9/DDP and HSC-3/DDP cells (Fig. 4I and J). Taken together, these results suggested that silencing of miR-27b-3p partly reversed the promotion effect of OIP5-AS1 knockdown on DDP sensitivity in DDP-resistant OSCC cells.

TRIM14 is a target of miR-27b-3p. It has been widely reported that miRNA can perform its function by specifically binding to the 3'-UTR of the downstream gene (29). Using the web-based tool starBase, the 3'-UTR of TRIM14 was found to have complementary target sites to miR-27b-3p (Fig. 5A). To verify this prediction, a dual-luciferase reporter assay was conducted in SCC-9/DDP and HSC-3/DDP cells. The results demonstrated that the luciferase activity was significantly decreased in cells

co-transfected with TRIM14 3'-UTR-WT and miR-27b-3p, whereas there was little effect in cells co-transfected with TRIM14 3'-UTR-MUT and miR-27b-3p (Fig. 5B and C).

It was demonstrated that the mRNA and protein expression levels of TRIM14 were significantly upregulated in OSCC tumor tissues compared with normal adjacent tissues (Fig. 5D and E, respectively). Moreover, TRIM14 was expressed at a higher level in SCC-9/DDP and HSC-3/DDP cells compared with SCC-9 and HSC-3 cells (Fig. 5F and G). It was found that TRIM14 expression was moderately negatively correlated with the expression of miR-27b-3p in OSCC tumor tissues (Fig. 5H).

The transfection efficiency of miR-27b-3p overexpression or knockdown was examined and presented in Fig. S1A. RT-qPCR and western blotting results indicated that at both the mRNA (Fig. 5I and J) and protein (Fig. 5K and L) levels TRIM14 expression was significantly decreased after miR-27b-3p overexpression, whereas expression levels were increased by anti-miR-27b-3p transfection in SCC-9/DDP and

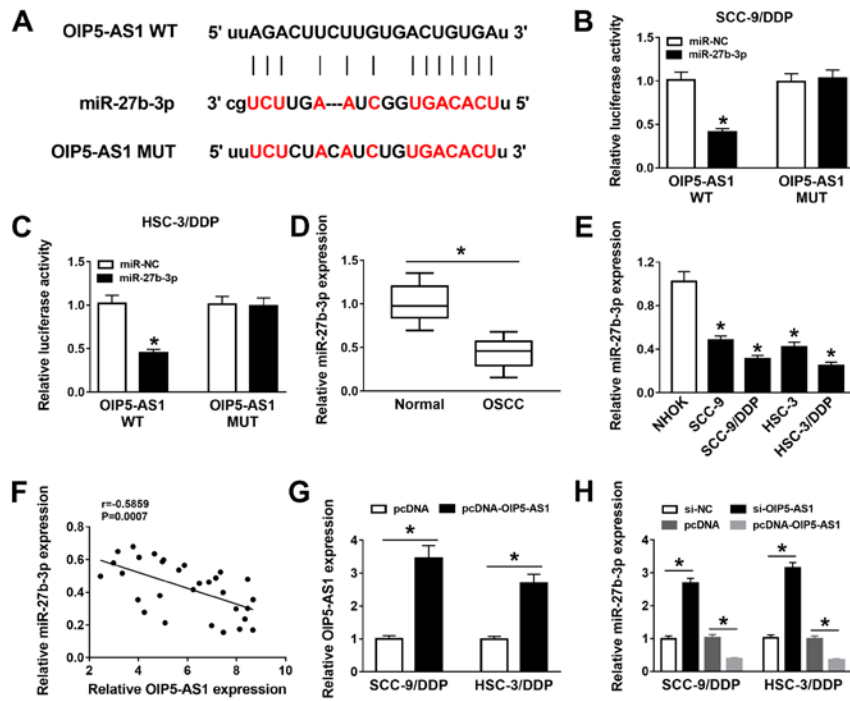


Figure 3. miR-27b-3p is a target of OIP5-AS1. (A) Binding sites between OIP5-AS1 and miR-27b-3p were predicted using starBase 2.0 software. Effects of miR-27b-3p overexpression on luciferase activity of OIP5-AS1 WT and OIP5-AS1 MUT reporters were measured by dual-luciferase reporter assay in (B) SCC-9/DDP and (C) HSC-3/DDP. (D) miR-27b-3p expression was detected using RT-qPCR in 30 pairs of OSCC tumor tissues and normal adjacent tissues. (E) miR-27b-3p expression in NHOK, SCC-9, SCC-9/DDP and HSC-3/DDP cells was assessed by RT-qPCR. (F) Correlation between OIP5-AS1 and miR-27b-3p expression levels in OSCC tissues was analyzed using Pearson correlation analysis. (G) OIP5-AS1 expression was measured in SCC-9/DDP and HSC-3/DDP cells transfected with pcDNA and pcDNA-OIP5-AS1. (H) RT-qPCR was performed to assess the expression levels of miR-27b-3p in SCC-9/DDP and HSC-3/DDP cells transfected with si-NC, si-OIP5-AS1, pcDNA or pcDNA-OIP5-AS1. * $P < 0.05$ vs. si-NC or pcDNA. DDP, cisplatin; siRNA, small interfering RNA; miR, microRNA; MUT, mutant; NC, negative control; OIP5-AS1, opa-interacting protein 5 antisense RNA 1; OSCC, oral squamous cell carcinoma; RT-qPCR, reverse transcription-quantitative PCR; WT, wild-type.

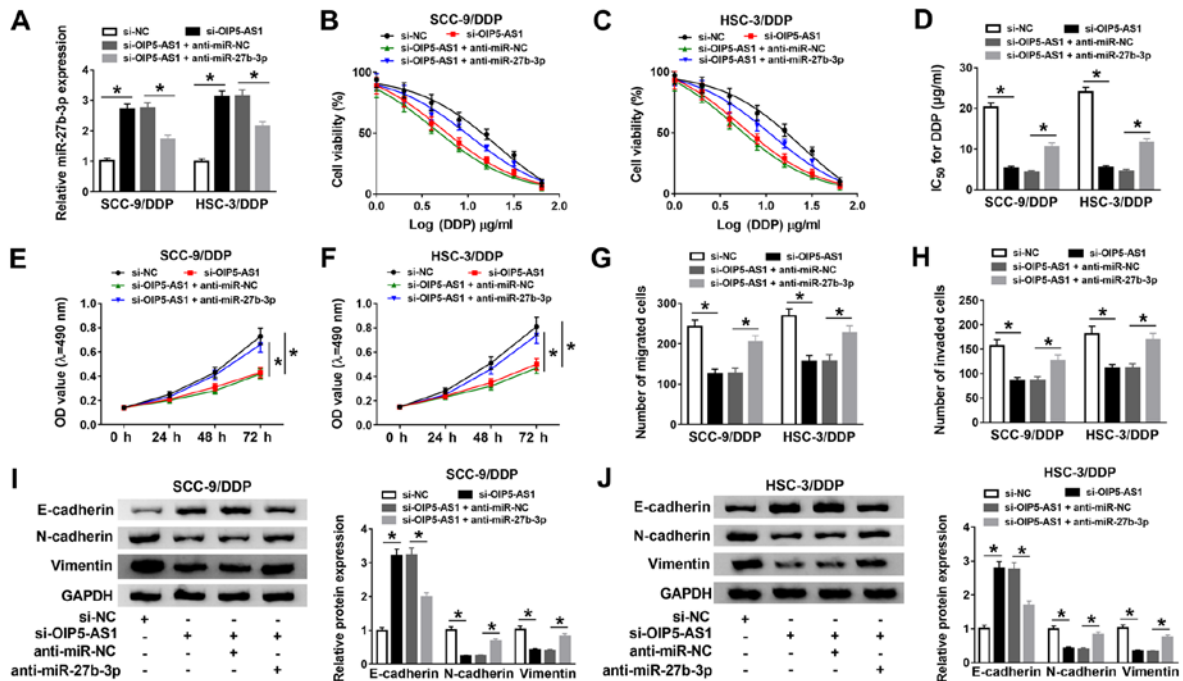


Figure 4. OIP5-AS1 knockdown improves DDP sensitivity in DDP-resistant oral squamous cell carcinoma cells by negatively regulating miR-27b-3p. (A) miR-27b-3p expression was detected using reverse transcription-quantitative PCR in SCC-9/DDP and HSC-3/DDP cells transfected with si-NC, si-OIP5-AS1, si-OIP5-AS1 + anti-miR-NC or si-OIP5-AS1 + anti-miR-27b-3p. (B and C) Transfected SCC-9/DDP and HSC-3/DDP cells were treated with various doses of DDP for 48 h. And then, MTT assay was performed to measure cell viability in treated cells. (D) The viability curve was applied to calculate the IC_{50} . Proliferation in transfected (E) SCC-9/DDP and (F) HSC-3/DDP cells was assessed using a MTT assay. (G) Migration and (H) invasion in transfected SCC-9/DDP and HSC-3/DDP cells were measured by Transwell and Matrigel assays, respectively. Protein expression levels of E-cadherin, N-cadherin and Vimentin in transfected (I) SCC-9/DDP and (J) HSC-3/DDP cells were detected by western blot analysis. * $P < 0.05$ vs. si-NC or si-OIP5-AS1 + anti-miR-NC. DDP, cisplatin; miR, microRNA; NC, negative control; OD, optical density; OIP5-AS1, opa-interacting protein 5 antisense RNA 1; siRNA, small interfering RNA.

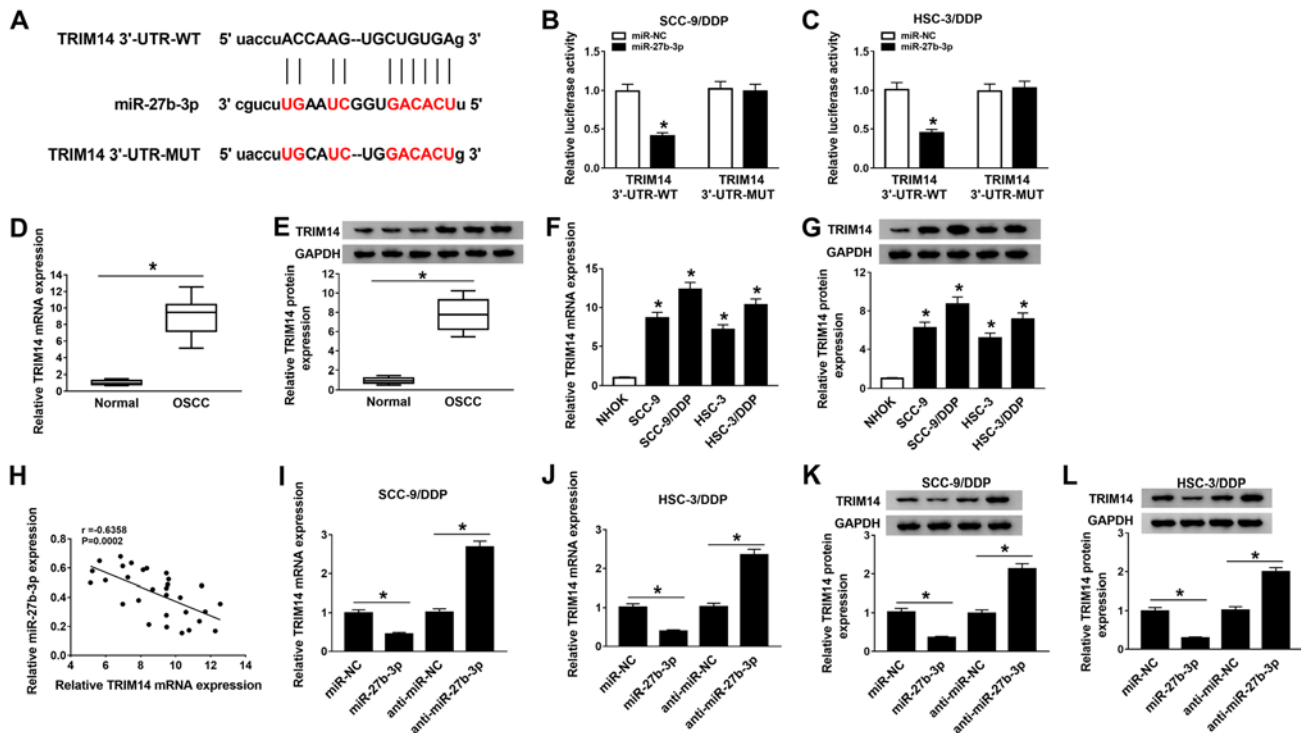


Figure 5. TRIM14 is a direct target of miR-27b-3p. (A) Putative binding sites between miR-27b-3p and TRIM14 3'-UTR were predicted using starBase 2.0 software. Relative luciferase activity was determined using dual-luciferase reporter assays in (B) SCC-9/DDP and (C) HSC-3/DDP cells co-transfected with reporter plasmid (TRIM14 3'-UTR-WT or TRIM14 3'-UTR-MUT) and miR-27b-3p or miR-NC. (D) mRNA and (E) protein expression levels of TRIM14 in 30 pairs of OSCC tumor tissues and normal adjacent tissues were measured using RT-qPCR and western blot analysis, respectively; representative western blotting images of three normal and three tumoral tissues are presented. (F) RT-qPCR and (G) western blotting were conducted to evaluate the mRNA and protein expression levels of TRIM14 in NHOK, SCC-9, HSC-3, SCC-9/DDP and HSC-3/DDP cells. (H) Pearson correlation analysis was performed to determine the correlation between miR-27b-3p and TRIM14 expression levels in OSCC tissues. TRIM14 mRNA expression was assessed by RT-qPCR in transfected (I) SCC-9/DDP and (J) HSC-3/DDP cells transfected with miR-NC, miR-27b-3p, anti-miR-NC or anti-miR-27b-3p. TRIM14 protein expression was examined using western blotting in transfected (K) SCC-9/DDP and (L) HSC-3/DDP cells. * $P < 0.05$ vs. miR-NC or anti-miR-NC. DDP, cisplatin; miR, microRNA; MUT, mutant; NC, negative control; NHOK, normal human oral keratinocyte; OIP5-AS1, opa-interacting protein 5 antisense RNA 1; OSCC, oral squamous cell carcinoma; RT-qPCR, reverse transcription-quantitative PCR; TRIM14, tripartite motif-containing 14; UTR, untranslated region; WT, wild-type.

HSC-3/DDP cells. Therefore, it was suggested that miR-27b-3p could interact with TRIM14 to inhibit its expression.

TRIM14 overexpression partially reverses the effects of miR-27b-3p on DDP sensitivity in DDP-resistant OSCC cells. As miR-27b-3p was shown to negatively regulate TRIM14 expression, whether the effect of miR-27b-3p on DDP sensitivity was mediated by regulating TRIM14 expression was investigated. The overexpression of miR-27b-3p decreased TRIM14 expression, which was significantly reversed by co-transfection with TRIM14 overexpression vectors in SCC-9/DDP and HSC-3/DDP cells (Fig. 6A-C). The overexpression efficiency of pcDNA-TRIM14 was examined and presented in Fig. S1B and SC.

The IC₅₀ value of DDP suggested that the overexpression of TRIM14 effectively abolished the suppressive effect of miR-27b-3p mimic on DDP resistance in SCC-9/DDP and HSC-3/DDP cells (Fig. 6D-F). Moreover, transfection of miR-27b-3p inhibited the proliferation (Fig. 6G and H), migration (Figs. 6I and S2C) and invasion (Figs. 6J and S2D) in SCC-9/DDP and HSC-3/DDP cells, and the overexpression of TRIM14 significantly reversed these effects. It was demonstrated that increased E-cadherin protein expression, as well as decreased N-cadherin and Vimentin protein expression levels induced by miR-27b-3p mimic were reversed by pcDNA-TRIM14 co-transfection in SCC-9/DDP and HSC-3/DDP cells (Fig. 6K and L). Thus, these

results suggested that miR-27b-3p may facilitate DDP sensitivity in DDP-resistant OSCC cells by regulating TRIM14.

OIP5-AS1 enhances TRIM14 expression by sponging miR-27b-3p in DDP-resistant OSCC cells. Based on the aforementioned findings, it was hypothesized that OIP5-AS1 may affect the expression of TRIM14 by modulating miR-27b-3p in DDP-resistant OSCC cells. A moderate positive correlation was identified between OIP5-AS1 and TRIM14 expression levels (Fig. 7A). RT-qPCR results demonstrated that knockdown of OIP5-AS1 decreased TRIM14 expression, and introduction of anti-miR-27b-3p effectively reversed this trend in SCC-9/DDP and HSC-3/DDP cells (Fig. 7B). Similar to the RT-qPCR results, the protein expression levels of TRIM14 were significantly suppressed in si-OIP5-AS1-transfected SCC-9/DDP and HSC-3/DDP cells, whereas silencing of miR-27b-3p mitigated this inhibitory effect of OIP5-AS1 knockdown (Fig. 7C and D). Taken together, these results suggested that OIP5-AS1 may serve as a molecular sponge of miR-27b-3p to upregulate TRIM14 expression in DDP-resistant OSCC cells.

OIP5-AS1 knockdown increases DDP sensitivity of OSCC in vivo. To further evaluate the functional effects of OIP5-AS1 on DDP resistance *in vivo*, a mouse xenograft model of OSCC was established. The knockdown efficiency of sh-OIP5-AS1

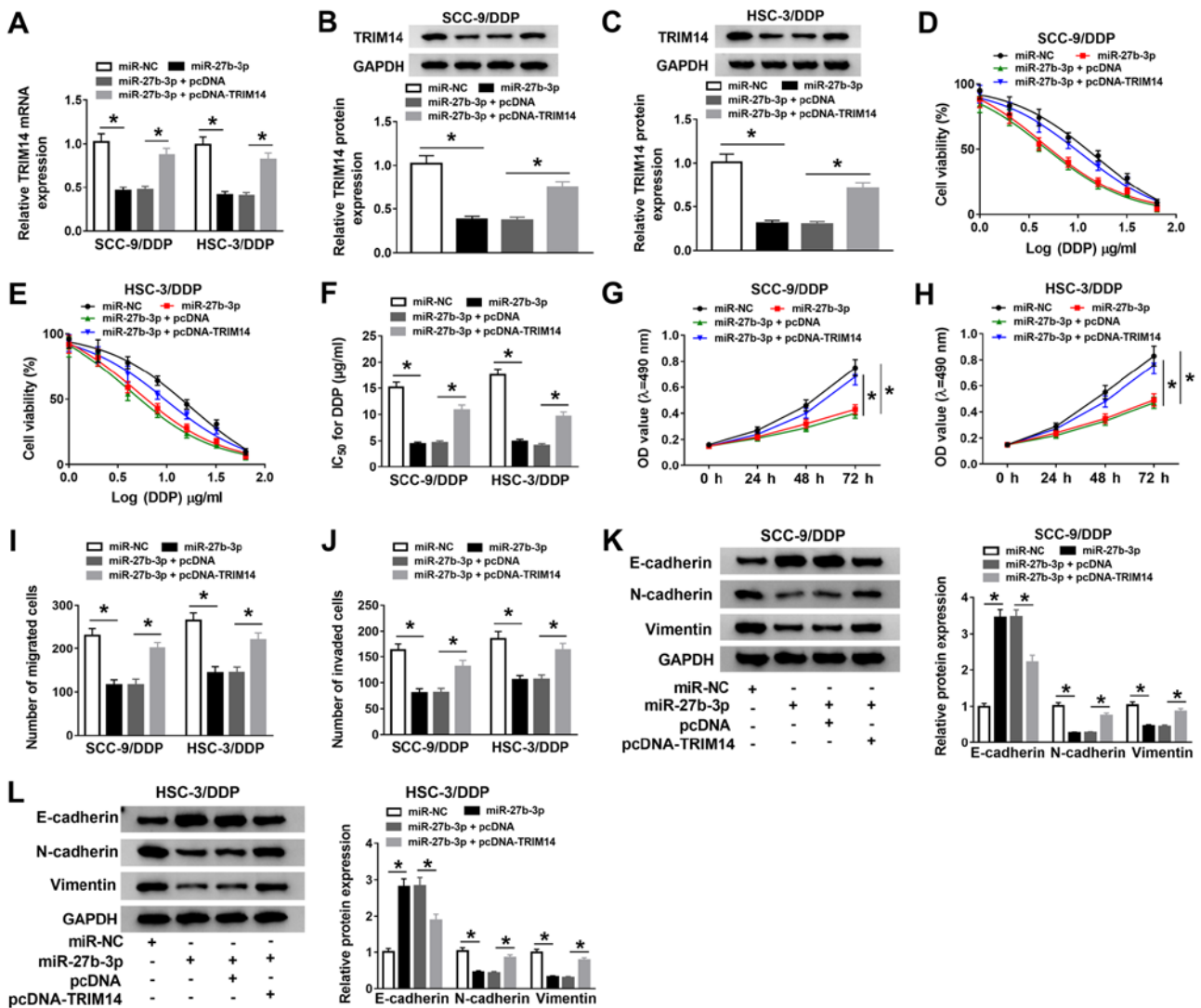


Figure 6. TRIM14 overexpression partly reverses the effects of miR-27b-3p on DDP sensitivity in DDP-resistant oral squamous cell carcinoma cells. (A) Reverse transcription-quantitative PCR was conducted to detect the mRNA expression levels of TRIM14 in SCC-9/DDP and HSC-3/DDP cells transfected with miR-NC, miR-27b-3p, miR-27b-3p + pcDNA or miR-27b-3p + pcDNA-TRIM14. Western blotting was performed to assess the protein expression level of TRIM14 in transfected (B) SCC-9/DDP and (C) HSC-3/DDP cells. (D and E) Transfected SCC-9/DDP and HSC-3/DDP cells were treated with various concentrations of DDP for 48 h. MTT assay was subsequently carried out to assess cell viability in treated cells. (F) The viability curve was used to calculate the IC_{50} . MTT assay was performed to test proliferation rates in transfected (G) SCC-9/DDP and (H) HSC-3/DDP cells. Transwell and Matrigel assays were used to measure (I) migration and (J) invasion, respectively, in transfected SCC-9/DDP and HSC-3/DDP cells. Western blotting was conducted to assess the protein expression levels of E-cadherin, N-cadherin and Vimentin in transfected (K) SCC-9/DDP and (L) HSC-3/DDP cells. * $P < 0.05$. DDP, cisplatin; miR, microRNA; NC, negative control; OD, optical density; OIP5-AS1, opa-interacting protein 5 antisense RNA 1; TRIM14, tripartite motif-containing 14.

in SCC-9 cells was measured and presented in Fig. S1D. The results demonstrated that the tumor size and weight were significantly lower in the sh-OIP5-AS1 group treated DDP compared with the sh-NC group treated DDP, indicating that OIP5-AS1 knockdown hindered tumor growth in OSCC *in vivo* (Fig. 8A and B). Furthermore, RT-qPCR and western blotting results revealed that OIP5-AS1 mRNA (Fig. 8C) and TRIM14 mRNA and protein (Fig. 8E and F, respectively) expression levels were decreased, whereas miR-27b-3p expression was enhanced (Fig. 8D) in tumor tissues from mice injected with sh-OIP5-AS1-transfected SCC-9 cells compared with mice injected with sh-NC-transfected SCC-9 cells. Collectively, these results indicated that knockdown of OIP5-AS1 repressed tumor growth and enhanced DDP sensitivity partly by regulating the miR-27b-3p/TRIM14 axis in OSCC *in vivo*.

Discussion

DDP-based chemotherapy is effective in the clinical treatment of most cancer types, but the development of drug resistance leads to poor clinical effectiveness (30). Previous studies have reported that lncRNAs are essential regulators in development and drug resistance of various cancer types (31,32). For example, it was previously reported that the high expression of OIP5-AS1 was associated with undifferentiated oral tumors and indicated a poor prognosis (33). Furthermore, it has been shown that OIP5-AS1 knockdown can reduce the resistance of osteosarcoma cells to DDP (10). However, the mechanism of OIP5-AS1 in DDP resistance is yet to be fully elucidated in OSCC.

In the present study, OIP5-AS1 was demonstrated to be highly expressed in DDP-resistant OSCC cells compared with parental cells, suggesting that OIP5-AS1 may exert an

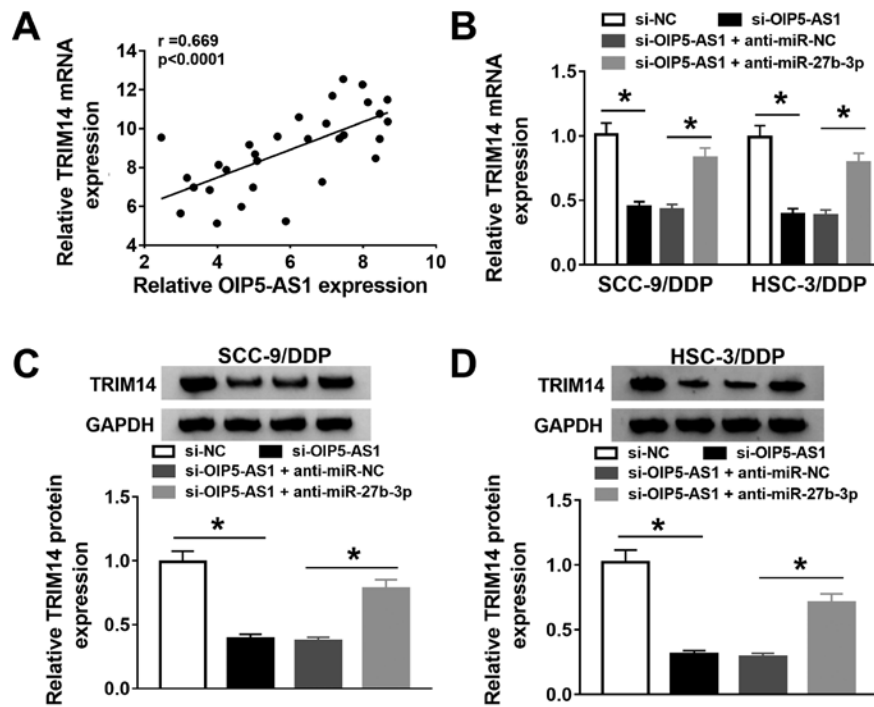


Figure 7. OIP5-AS1 elevates TRIM14 expression by sponging miR-27b-3p in DDP-resistant oral squamous cell carcinoma cells. (A) Pearson correlation analysis was used to analyze the correlation between OIP5-AS1 and TRIM14 expression levels in OSCC tissues. (B) TRIM14 mRNA expression was detected by RT-qPCR assay in SCC-9/DDP and HSC-3/DDP cells transfected with si-NC, si-OIP5-AS1, si-OIP5-AS1 + anti-miR-NC or si-OIP5-AS1 + anti-miR-27b-3p. TRIM14 protein expression was measured using western blotting in transfected (C) SCC-9/DDP and (D) HSC-3/DDP cells. * $P < 0.05$. DDP, cisplatin; miR, microRNA; NC, negative control; OIP5-AS1, opa-interacting protein 5 antisense RNA 1; siRNA, small interfering RNA; TRIM14, tripartite motif-containing 14.

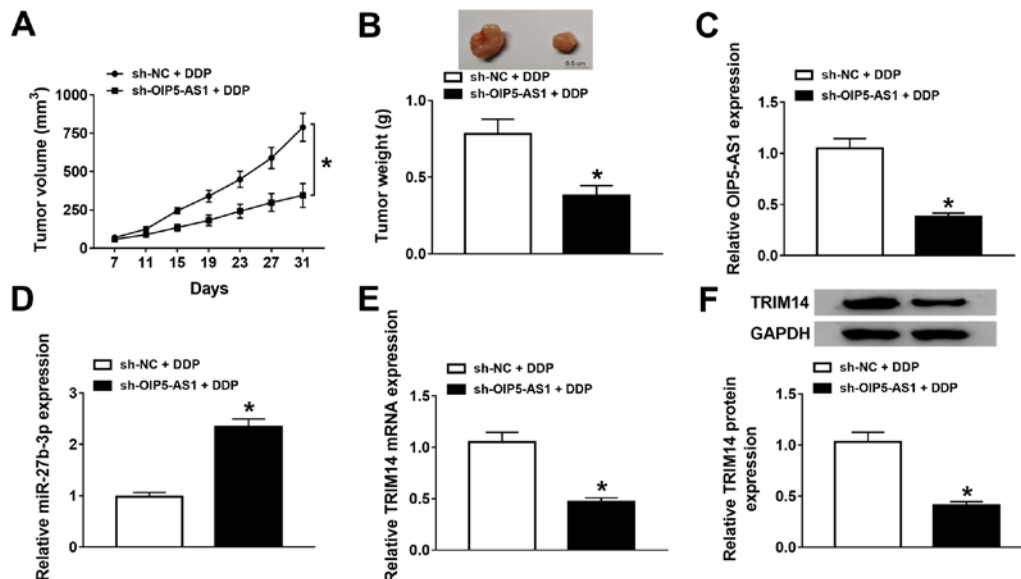


Figure 8. OIP5-AS1 knockdown improves DDP sensitivity of OSCC *in vivo*. (A) Tumor volume and (B) tumor weight were measured in xenografts. (C) OIP5-AS1 and (D) miR-27b-3p expression levels were measured in xenografts using RT-qPCR. TRIM14 mRNA and protein expression levels in xenografts was assessed by (E) RT-qPCR and (F) western blot analysis, respectively. * $P < 0.05$ vs. sh-NC + DDP. DDP, cisplatin; miR, microRNA; NC, negative control; OIP5-AS1, opa-interacting protein 5 antisense RNA 1; shRNA, short hairpin RNA; TRIM14, tripartite motif-containing 14.

oncogenic role in the DDP chemoresistance of OSCC cells. Subsequently, the biological function of OIP5-AS1 on DDP resistance in OSCC cells was further evaluated. The results showed that OIP5-AS1 knockdown increased DDP sensitivity and repressed proliferation, migration, invasion and EMT in DDP-resistant OSCC cells *in vitro*. Moreover, the current study

demonstrated that knockdown of OIP5-AS1 hindered OSCC cell growth, and improved DDP sensitivity *in vivo*. Therefore, it was suggested that OIP5-AS1 knockdown may contribute to DDP sensitivity *in vitro* and *in vivo*.

Previous studies have revealed that lncRNAs can exert their roles by interacting with miRNA (34,35). In the present study,

miR-27b-3p was demonstrated to be a target A of OIP5-AS1. It has been shown that miR-27b-3p could exert an inductive effect on drug sensitivity in breast cancer (17). The present results indicated that miR-27b-3p expression was downregulated and negatively correlated with the expression of OIP5-AS1 in OSCC tissues and DDP-resistant OSCC cells. Functionally, silencing miR-27b-3p reversed OIP5-AS1-knockdown-induced enhancement of DDP sensitivity, demonstrating that the knockdown of OIP5-AS1 increased DDP sensitivity partly by interacting with miR-27b-3p in DDP-resistant OSCC cells.

lncRNAs may act as sponges to reduce mRNA expression (27,36). In the present research, TRIM14 was identified as the target of miR-27b-3p using bioinformatics analysis and dual-luciferase reporter assays. According to previous literature, TRIM14 can affect the activity of Wnt/ β -catenin to promote the drug resistance of tumors (23). Moreover, the Wnt/ β -catenin signaling pathway contributes to oxaliplatin (OXA) resistance of liver cancer by enhancing the expression of multidrug resistance mutation 1 (MDR1) (37), and the Wnt/ β -catenin signaling pathway increases DDP resistance of lung adenocarcinoma by increasing the expression of ATP-binding cassette (ABC) transporter (38). Therefore, we hypothesize that TRIM14 could induce ABC transporter and MDR1 expression by activating the Wnt/ β -catenin signaling pathway, thus enhancing OSCC resistance to DDP.

Previous studies have reported that TRIM14 could increase progression in OSCC and enhance DDP resistance in oral tongue squamous cell cancer (21,22). The present study results demonstrated that TRIM14 was upregulated, and inversely correlated with miR-27b-3p level in OSCC. Functional analysis demonstrated that TRIM14 overexpression reserved the promotion role of miR-27b-3p on DDP sensitivity. The inductive effect of TRIM14 on DDP resistance was also verified in tongue squamous cell carcinoma (39). Additionally, to further assess whether OIP5-AS1 could act as a miR-27b-3p sponge to impact TRIM14 expression, rescue assays were conducted. In the present study, the results demonstrated that the down-regulation of miR-27b-3p could partly reversed the suppressive action of OIP5-AS1 knockdown on TRIM14 expression in DDP-resistant OSCC cells, verifying the regulatory role of OIP5-AS1/miR-27b-3p/TRIM14 in OSCC. The current study is limited by the small sample size and the verification of other associated signaling pathways (23). Therefore, in future studies, the sample size should be expanded, and whether the regulatory role of OIP5-AS1/miR-27b-3p/TRIM14 axis on DDP resistance was mediated by the Wnt/ β -catenin signaling pathway should be explored further.

In conclusion, the present results suggested that OIP5-AS1 may act as a sponge of miR-27b-3p to upregulate TRIM14 expression, thus promoting DDP resistance of OSCC cells. Therefore, targeting OIP5-AS1 maybe a potential therapeutic target for OSCC treatment.

Acknowledgements

Not applicable.

Funding

No funding was received.

Availability of data and materials

The datasets used and/or analyzed during the current study are available from the corresponding author on reasonable request.

Authors' contributions

ZX conceived and designed the study. JL, QJ and DL performed the experiments, and performed data mining, acquisition and analysis. ZX wrote and approved the final manuscript. All authors read and approved the final manuscript.

Ethical approval and consent to participate

The study was performed with the approval of the Ethical Committee of The First Hospital of Qiqihar (Qiqihar, China). Written informed consents were obtained from every participant. The animal experiments were performed as per the protocol approved by the Institutional Committee for Animal Research of The First Hospital of Qiqihar.

Patient consent for publication

Not applicable.

Competing interests

The authors declare that they have no competing interests.

References

1. Jin LJ, Lamster IB, Greenspan JS, Pitts NB, Scully C and Warnakulasuriya S: Global burden of oral diseases: Emerging concepts, management and interplay with systemic health. *Oral Dis* 22: 609-619, 2016.
2. Bray F, Ferlay J, Soerjomataram I, Siegel RL, Torre LA and Jemal A: Global cancer statistics 2018: GLOBOCAN estimates of incidence and mortality worldwide for 36 cancers in 185 countries. *CA Cancer J Clin* 68: 394-424, 2018.
3. Montero PH and Patel SG: Cancer of the oral cavity. *Surg Oncol Clin N Am* 24: 491-508, 2015.
4. Troiano G, Mastrangelo F, Caponio VCA, Laino L, Cirillo N and Lo Muzio L: Predictive prognostic value of tissue-based MicroRNA expression in oral squamous cell carcinoma: A systematic review and meta-analysis. *J Dent Res* 97: 759-766, 2018.
5. Wang D and Lippard SJ: Cellular processing of platinum anticancer drugs. *Nat Rev Drug Discov* 4: 307-320, 2005.
6. Ma L, Bajic VB and Zhang Z: On the classification of long non-coding RNAs. *RNA Biol* 10: 925-933, 2013.
7. Wang Y, Zhang X, Wang Z, Hu Q, Wu J, Li Y, Ren X, Wu T, Tao X, Chen X, *et al*: lncRNA-p23154 promotes the invasion-metastasis potential of oral squamous cell carcinoma by regulating Glut1-mediated glycolysis. *Cancer Lett* 434: 172-183, 2018.
8. Zhang C, Bao C, Zhang X, Lin X, Pan D and Chen Y: Knockdown of lncRNA LEF1-AS1 inhibited the progression of oral squamous cell carcinoma (OSCC) via Hippo signaling pathway. *Cancer Biol Ther* 20: 1213-1222, 2019.
9. Li M, Ning J, Li Z, Fei Q, Zhao C, Ge Y and Wang L: Long noncoding RNA OIP5-AS1 promotes the progression of oral squamous cell carcinoma via regulating miR-338-3p/NRP1 axis. *Biomed Pharmacother* 118: 109259, 2019.
10. Song L, Zhou Z, Gan Y, Li P, Xu Y, Zhang Z, Luo F, Xu J, Zhou Q and Dai F: Long noncoding RNA OIP5-AS1 causes cisplatin resistance in osteosarcoma through inducing the LPAATbeta/PI3K/AKT/mTOR signaling pathway by sponging the miR-340-5p. *J Cell Biochem* 120: 9656-9666, 2019.

11. Hammond SM: An overview of microRNAs. *Adv Drug Deliv Rev* 87: 3-14, 2015.
12. Nagai H, Hasegawa S, Uchida F, Terabe T, Ishibashi Kanno N, Kato K, Yamagata K, Sakai S, Kawashiri S, Sato H, *et al*: MicroRNA-205-5p suppresses the invasiveness of oral squamous cell carcinoma by inhibiting TIMP2 expression. *Int J Oncol* 52: 841-850, 2018.
13. Feng X, Luo Q, Wang H, Zhang H and Chen F: MicroRNA-22 suppresses cell proliferation, migration and invasion in oral squamous cell carcinoma by targeting NLRP3. *J Cell Physiol* 233: 6705-6713, 2018.
14. Peng M and Pang C: MicroRNA-140-5p inhibits the tumorigenesis of oral squamous cell carcinoma by targeting p21-activated kinase 4. *Cell Biol Int*: Aug 8, 2019 (Epub ahead of print). doi: 10.1002/cbin.11213. 2019.
15. Fukumoto I, Koshizuka K, Hanazawa T, Kikkawa N, Matsushita R, Kurozumi A, Kato M, Okato A, Okamoto Y and Seki N: The tumor-suppressive microRNA-23b/27b cluster regulates the MET oncogene in oral squamous cell carcinoma. *Int J Oncol* 49: 1119-1129, 2016.
16. Liu B, Chen W, Cao G, Dong Z, Xu J, Luo T and Zhang S: MicroRNA-27b inhibits cell proliferation in oral squamous cell carcinoma by targeting FZD7 and Wnt signaling pathway. *Arch Oral Biol* 83: 92-96, 2017.
17. Zhu J, Zou Z, Nie P, Kou X, Wu B, Wang S, Song Z and He J: Downregulation of microRNA-27b-3p enhances tamoxifen resistance in breast cancer by increasing NR5A2 and CREB1 expression. *Cell Death Dis* 7: e2454, 2016.
18. Zhang G, Tian X, Li Y, Wang Z, Li X and Zhu C: miR-27b and miR-34a enhance docetaxel sensitivity of prostate cancer cells through inhibiting epithelial-to-mesenchymal transition by targeting ZEB1. *Biomed Pharmacother* 97: 736-744, 2018.
19. Liu B, Cao G, Dong Z and Guo T: Effect of microRNA-27b on cisplatin chemotherapy sensitivity of oral squamous cell carcinoma via FZD7 signaling pathway. *Oncol Lett* 18: 667-673, 2019.
20. Nenashva VV, Nikolaev AI, Martynenko AV, Kaplanskaya IB, Bodemer W, Hunsmann G and Tarantul VZ: Differential gene expression in HIV/SIV-associated and spontaneous lymphomas. *Int J Med Sci* 2: 122-128, 2005.
21. Wang T, Ren Y, Liu R, Ma J, Shi Y, Zhang L and Bu R: miR-195-5p suppresses the proliferation, migration, and invasion of oral squamous cell carcinoma by targeting TRIM14. *Biomed Res Int* 2017: 7378148, 2017.
22. Wang X, Guo H, Yao B and Helms J: miR-15b inhibits cancer-initiating cell phenotypes and chemoresistance of cisplatin by targeting TRIM14 in oral tongue squamous cell cancer. *Oncol Rep* 37: 2720-2726, 2017.
23. Tan Z, Song L, Wu W, Zhou Y, Zhu J, Wu G, Cao L, Song J, Li J and Zhang W: TRIM14 promotes chemoresistance in gliomas by activating Wnt/ β -catenin signaling via stabilizing Dvl2. *Oncogene* 37: 5403-5415, 2018.
24. Song L, Duan P, Gan Y, Li P, Zhao C, Xu J, Zhang Z and Zhou Q: Silencing LPAAT β inhibits tumor growth of cisplatin-resistant human osteosarcoma *in vivo* and *in vitro*. *Int J Oncol* 50: 535-544, 2017.
25. Livak KJ and Schmittgen TD: Analysis of relative gene expression data using real-time quantitative PCR and the 2(-Delta Delta C(T)) method. *Methods* 25: 402-408, 2001.
26. Xu W, Chang J, Du X and Hou J: Long non-coding RNA PCAT-1 contributes to tumorigenesis by regulating FSCN1 via miR-145-5p in prostate cancer. *Biomed Pharmacother* 95: 1112-1118, 2017.
27. Li S, Chen X, Liu X, Yu Y, Pan H, Haak R, Schmidt J, Ziebolz D and Schmalz G: Complex integrated analysis of lncRNAs-miRNAs-mRNAs in oral squamous cell carcinoma. *Oral Oncol* 73: 1-9, 2017.
28. Schober P, Boer C and Schwarte LA: Correlation coefficients: Appropriate use and interpretation. *Anesth Analg* 126: 1763-1768, 2018.
29. Winter J, Jung S, Keller S, Gregory RI and Diederichs S: Many roads to maturity: MicroRNA biogenesis pathways and their regulation. *Nat Cell Biol* 11: 228-234, 2009.
30. Stordal B, Pavlakis N and Davey R: A systematic review of platinum and taxane resistance from bench to clinic: An inverse relationship. *Cancer Treat Rev* 33: 688-703, 2007.
31. Fang Z, Chen W, Yuan Z, Liu X and Jiang H: LncRNA-MALAT1 contributes to the cisplatin-resistance of lung cancer by upregulating MRP1 and MDR1 via STAT3 activation. *Biomed Pharmacother* 101: 536-542, 2018.
32. Fang Z, Zhao J, Xie W, Sun Q, Wang H and Qiao B: LncRNA UCA1 promotes proliferation and cisplatin resistance of oral squamous cell carcinoma by suppressing miR-184 expression. *Cancer Med* 6: 2897-2908, 2017.
33. Arunkumar G, Anand S, Raksha P, Dhamodharan S, Prasanna Srinivasa Rao H, Subbiah S, Murugan AK and Munirajan AK: LncRNA OIP5-AS1 is overexpressed in undifferentiated oral tumors and integrated analysis identifies a downstream effector of stemness-associated transcription factors. *Sci Rep* 8: 7018, 2018.
34. Sun CC, Zhang L, Li G, Li SJ, Chen ZL, Fu YF, Gong FY, Bai T, Zhang DY, Wu QM and Li DJ: The lncRNA PDIA3P interacts with miR-185-5p to modulate oral squamous cell carcinoma progression by targeting cyclin D2. *Mol Ther Nucleic Acids* 9: 100-110, 2017.
35. Chang SM and Hu WW: Long non-coding RNA MALAT1 promotes oral squamous cell carcinoma development via microRNA-125b/STAT3 axis. *J Cell Physiol* 233: 3384-3396, 2018.
36. Zhou RS, Zhang EX, Sun QF, Ye ZJ, Liu JW, Zhou DH and Tang Y: Integrated analysis of lncRNA-miRNA-mRNA ceRNA network in squamous cell carcinoma of tongue. *BMC Cancer* 19: 779, 2019.
37. Cao F and Yin LX: miR-122 enhances sensitivity of hepatocellular carcinoma to oxaliplatin via inhibiting MDR1 by targeting Wnt/ β -catenin pathway. *Exp Mol Pathol* 106: 34-43, 2019.
38. Wang Q, Geng F, Zhou H, Chen Y, Du J, Zhang X, Song D and Zhao H: MDIG promotes cisplatin resistance of lung adenocarcinoma by regulating ABC transporter expression via activation of the WNT/ β -catenin signaling pathway. *Oncol Lett* 18: 4294-4307, 2019.
39. Qiao CY, Qiao TY, Jin H, Liu LL, Zheng MD and Wang ZL: LncRNA KCNQ1OT1 contributes to the cisplatin resistance of tongue cancer through the KCNQ1OT1/miR-124-3p/TRIM14 axis. *Eur Rev Med Pharmacol Sci* 241: 200-212, 2020.



This work is licensed under a Creative Commons Attribution-NonCommercial-NoDerivatives 4.0 International (CC BY-NC-ND 4.0) License.